NASA TN D-686

NASA TN D-686

# TECHNICAL NOTE
## D-686

LARGE-SCALE WIND-TUNNEL TESTS OF EXHAUST INGESTION DUE TO THRUST REVERSAL ON A FOUR-ENGINE JET TRANSPORT DURING GROUND ROLL

By William H. Tolhurst, Jr., David H. Hickey, and Kiyoshi Aoyagi

Ames Research Center
Moffett Field, Calif.

NATIONAL AERONAUTICS AND SPACE ADMINISTRATION
WASHINGTON January 1961

NATIONAL AERONAUTICS AND SPACE ADMINISTRATION

---

TECHNICAL NOTE D-686

---

# LARGE-SCALE WIND-TUNNEL TESTS OF EXHAUST INGESTION DUE TO THRUST REVERSAL ON A FOUR-ENGINE JET TRANSPORT DURING GROUND ROLL

By William H. Tolhurst, Jr., David H. Hickey,
and Kiyoshi Aoyagi

## SUMMARY

Wind-tunnel tests have been conducted on a large-scale model of a swept-wing jet transport type airplane to study the factors affecting exhaust gas ingestion into the engine inlets when thrust reversal is used during ground roll. The model was equipped with four small jet engines mounted in nacelles beneath the wing. The tests included studies of both cascade and target type reversers.

The data obtained included the free-stream velocity at the occurrence of exhaust gas ingestion in the outboard engine and the increment of drag due to thrust reversal for various modifications of thrust reverser configuration. Motion picture films of smoke flow studies were also obtained to supplement the data.

The results show that the free-stream velocity at which ingestion occurred in the outboard engines could be reduced considerably, by simple modifications to the reversers, without reducing the effective drag due to reversed thrust.

## INTRODUCTION

Several studies have been made at the Ames Research Center of the effect of thrust reversal on the flight characteristics of single-engined jet airplanes during landing approach. The results of wind-tunnel studies on full-scale airplanes were reported in references 1 and 2 and the results of flight tests in reference 3. The wind-tunnel studies have been extended to include the effects of thrust reversal on a four-engined subsonic jet transport-type airplane.

The present study was made to determine the exhaust gas ingestion characteristics of thrust reversers during ground roll. Tests were conducted with a large-scale jet transport model described in reference 4. Either cascade-type or target-type thrust reversers were mounted on small jet engines to determine the free-stream velocity at which exhaust gas would enter the engine inlets for various modificiations of the thrust reversers. Tests included the evaluation of simple methods which could reduce the velocity at ingestion and could be incorporated in thrust reversers of current design without unduly affecting the reverser effectiveness. The studies were made at the ground-roll height and were limited to determination of the velocities for ingestion between the inboard and outboard engines on one wing panel only. Although it was recognized that ingestion could occur from flow across the plane of symmetry, it was less likely than in the case chosen for study. The results are presented in terms of the velocity at ingestion and the over-all airplane drag change due to thrust reversal for various configurations of the thrust reversers and various engine powers. A motion picture film of smoke flow studies is available to supplement the data.

## NOTATION

$b$ wing span, ft

$\Delta C_D$ change in drag coefficient due to thrust reversal, $\frac{\Delta D}{q_\infty S}$

$\Delta D$ change in drag due to thrust reversal, drag force with reversed thrust minus drag force with engines off, lb

$c$ wing chord, ft

$\bar{c}$ wing mean aerodynamic chord, ft

$F_g$ forward thrust, lb

$-F_g$ reversed thrust, lb

$q_\infty$ free-stream dynamic pressure, lb/ft$^2$

$q_i$ free-stream dynamic pressure when ingestion first occurred and raised temperature in the inlet of the outboard engine, lb/ft$^2$

$q_t$ free-stream dynamic pressure when the outboard engine tail-pipe temperature indicated a sharp rise due to ingestion, lb/ft$^2$

$S$ wing area, ft$^2$

$V$ velocity, knots

$W_e$ engine intake weight rate of flow corrected to standard atmosphere, lb/sec

$\delta_f$ flap deflection angle, deg

$\delta_v$ vane or end-plate deflection angle measured from tail-pipe plane of symmetry, deg

Subscripts

A
4
4
5

$i$ ingestion

$m$ model

$F$ full scale

$t$ tail pipe

## MODEL AND APPARATUS

### Airplane

The model tested was a swept-wing jet transport type airplane with four jet engines installed in nacelles mounted on pylons beneath the wing. The wing had $35^{\circ}$ of sweepback measured on the quarter-chord line and an aspect ratio of 7.0. The model was the same one used in the tests reported in reference 4 and is described in detail in that report.

A sketch of the model and tunnel installation is shown in figure 1. The model was supported on short struts at a scale value of the distance of the airplane above the ground during roll. The ground plane was raised 4.5 inches above the tunnel floor as a protection for the tunnel floor and to remove some of the tunnel boundary layer. A photograph of the installation is shown in figure 2.

### Flaps

The outline of the wing trailing-edge flaps is shown in figure 1. The flaps were plain and of constant percent chord hinged at 68 percent of the streamwise chord. They extended spanwise from 0.09 to 0.34 and from 0.44 to 0.63 semispan.

## Thrust Reversers

Two types of thrust reversers were tested, the cascade-type reverser shown in figure 3 and the target type shown in figure 4. The opening on each side of the cascade reverser was divided into three horizontal sections, each containing a set of turning vanes. The vanes were pivoted to permit individual adjustment of the deflection angle.

The blocker plates, extending the full length of the vane sections, were used in various combinations to prevent flow through portions of the vane sections. Figure 3(a) shows the details of the outboard side of the reverser on the inboard engine with one blocker plate arrangement. The details of the reverser on the outboard engine were the same except that the blockers were mounted on the inboard side of the reverser. Throughout the test, blocker plates were attached to the upper half of the inboard upper section of each reverser to keep the hot exhaust gases away from the wing lower surface.

Figure 3(b) shows the details of the canted vane configuration which was used in place of the blockers to prevent direct mixing of the exhaust gas flow between the two engines. The normal vanes were removed from the mid-section of the outboard side of the inboard reverser only, and were replaced with vanes which were canted 45° with 40° vane deflection angle measured normal to the axis of vane rotation.

Details of the target-type reverser mounted on the outboard engine are shown in figure 4(a). The main sections of the reversers were fixed in the full-reverse position. The reverser support frame, not shown, permitted the reversers to be rotated and tilted. The distance between the tail pipe and reverser could be varied, but early in the test it was determined that a spacing of approximately 14 inches (ratio of spacing to tail-pipe diameter of 1.15) resulted in the most satisfactory engine operation; this spacing was therefore held constant for the remainder of the test. Flow dividers were installed in the apex of the reversers for flow stability, and deflector plates were added above and below the reverser to protect the wing and floor from direct flow of the exhaust gas.

The circular-arc end plates were pivoted to allow adjustment of the exhaust jet angle. The tabs, which served the same function as the blocker plates on the cascade reverser, were made of 1/8-inch steel plate welded to the end plate normal to the surface.

Details of the finned end plate and tapered end plate are shown in figure 4(b). The finned end plate was used only on the outboard side of the inboard engine while the tapered end plates were used on both engines. Figure 5 shows photographs of typical installations of both types of reversers.

## INSTRUMENTATION

The engine inlet temperature variation was measured by 7 thermocouples spaced symmetrically around the inside periphery of each engine inlet. The free-stream dynamic pressure was measured by a pitot-static tube mounted 5 feet above the tunnel floor and 29 feet ahead of the inboard engine inlet. The inlet temperatures, tail-pipe total temperature, and free-stream dynamic pressure were recorded simultaneously by an oscillograph. The weight rate of flow through each engine was determined from total head and static pressures measured at the engine inlet.

The exhaust gas flow was visualized by means of oil sprayed into the exhaust jet and was recorded by motion picture cameras mounted on the tunnel ceiling and floor ahead of the model.

The aerodynamic and thrust forces were measured by means of the standard wind-tunnel balance system.

## TESTS

### Range of Variables

The model was mounted on short, fixed struts at 0° angle of attack throughout the tests. The Reynolds number varied from 0 to $6.6\times10^6$ which corresponded to a maximum dynamic pressure of 25 pounds per square foot. The individual engine maximum gross thrust tested was approximately 900 pounds in forward thrust and 400 pounds in reverse thrust. The effect of thrust variation on the velocity at ingestion was determined for several configurations, but for the major portion of the test, the velocity at ingestion was determined with the engines operating at approximately two-thirds of the maximum thrust. Most of the tests were conducted with the wing trailing-edge flaps deflected to 50° but some data were obtained with the flaps undeflected. On the cascade reverser the vane deflection angle was varied from 35° to 55° and on the target reverser the end-plate deflection angle was varied from 25° to 35°.

### Procedure

The forward thrust of each engine was calibrated against the intake weight rate of flow. For each reversed thrust configuration the change in drag due to thrust reversal was determined at a free-stream dynamic pressure of 10 pounds per square foot at a constant engine thrust as determined by the weight rate of flow.

The highest free-stream dynamic pressure at which there was ingestion was determined with the engine weight rate of flow held at a constant value while the free-stream dynamic pressure was reduced from 25 pounds per square foot.

## CORRECTIONS

The scale measurements of reversed thrust ($-F_g$) have been corrected for the effects of airplane drag and ram drag. The engine weight rate of flow for each condition has been corrected to standard atmosphere.

A
4
4
5

## RESULTS

Since these tests were limited to the study of ingestion between the inboard and outboard engines, the data were obtained for the engines and reversers on one wing panel only. The values of $\Delta C_D$ and $F_g$ presented in the results are, however, in terms of four-engine operation except where noted. Exhaust gas ingestion occurred in the outboard engine intake before it occurred in the inboard engine; the results are therefore presented in terms of the highest free-stream dynamic pressure at which ingestion occurred in the outboard engine.

The values of forward static thrust measured without a reverser and the reversed static thrust for the cascade and target-type reversers are shown in figure 6.

For the purposes of these tests, ingestion is defined as occurring when an increase in the average temperature was indicated by any inlet thermocouple. Shown in figure 7 are records typical of the two types of variation of inlet temperatures, tail-pipe temperatures, and velocity with time as the velocity was decreased. The point where ingestion occurred is indicated on the record at the inlet temperature rise. Also indicated is the tail-pipe temperature rise which in some cases occurred at a much lower velocity than the velocity at which the temperature rise occurred in the inlet.

The results shown in table II give the measured free-stream dynamic pressure, $q_i$, and velocity, $V_i$, at which exhaust gas ingestion occurred for several values of engine thrust for each of four reverser configurations. The results indicate that, for each reverser configuration, the parameter, $-F_g/qS$, introduced in reference 1, is a correlating parameter for various values of model thrust. Therefore, values of ingestion velocity extrapolated to full-scale airplane thrust and wing area are included in the table. The use of $-F_g/qS$ as it applies to these tests is discussed in the appendix. The drag coefficient increment, $\Delta C_D$, given in the table is the change in drag coefficient due to thrust reversal, for each case, measured at a free-stream dynamic pressure of 10 pounds per square foot.

The results shown in table III(a) are for various configurations of cascade reversers, and in table III(b), for various configurations of target-type reversers and indicate the measured free-stream dynamic pressure at which ingestion occurred at the inlet and the dynamic pressure at which a large rate of change of tail-pipe temperature occurred. The corresponding velocities for ingestion for a typical transport airplane based on the correlating parameter discussed above indicate that the extrapolated full-scale values of ingestion velocity of above 80 knots for the basic reverser configurations can be reduced to about 40 knots by configuration changes which do not reduce the reverser effectiveness.

A445

The results shown in figure 8 show that the resultant drag coefficient change due to thrust reversal does not depend on the free-stream dynamic pressure at ingestion for the various configurations tested.

The results shown in figure 9 indicate the effect of trailing-edge flaps on the drag increment due to thrust reversal; when the trailing-edge flaps were deflected, the effective thrust reversal of the inboard engine was reduced considerably.

## QUALITATIVE OBSERVATIONS

The results of the ingestion studies that have been made are probably limited in scope to airplanes reasonably similar to the model tested in engine inlet geometry and reverser spacing as well as wing shape. However, it appears that certain general problem areas can be isolated by observations of the smoke patterns and the effect of the various modifications that were tested. A film supplement to the report shows typical smoke patterns for two configurations of the cascade reversers and two configurations of the target-type reversers.

For both types of reversers two factors of the same general nature influence reversed flow gas ingestion at relatively high ground-roll speeds. The first is that, in the plane of the inlets between the inboard and outboard engine, the exhaust gases from the two engines tend to penetrate each other and cause severe oscillations of the reversed flow stream and ingestion in either or both engine inlets. The second factor is the rebound of the exhaust gases from the ground into the outboard engine inlet. For both the cascade and the target-type reversers the use of blocker plates at the center line at the side of the reversers tended to split the reversed flow and, hence, prevented large mixing of gases in the plane of the inlets, thus delaying ingestion to lower velocities. Canted vanes on the outboard side of the inboard-engine cascade reverser and tapered end plates on the target-type reversers accomplished a similar purpose by directing the reversed flow gases from the two engines away from each other. For the second problem area, that of ground reflection, blocker plates in the lower portion of the reversers on both engine reversers aided in delaying or eliminating the ground bounce problem.

A third problem area that occurred with the cascade-type reversers only, and is probably due to the specific design of the reverser tail pipe and engine nacelle, was the occurrence of exhaust gas flow attachment to the nacelle and ingestion at high forward velocities. This was overcome by setting the first two rows of vanes next to the nacelle at relatively large angles and, hence, forcing the exhaust gas outward away from the nacelle.

Ames Research Center
National Aeronautics and Space Administration
Moffett Field, Calif., Oct. 26, 1960

A445

# APPENDIX

## PARAMETER USED TO SCALE MEASURED INGESTION VELOCITY TO FULL-SCALE VALUE

In order to utilize the large-scale model data for a full-scale airplane, tests were made to determine the effectiveness of the correlation parameter used in reference 1 which is the ratio of the momentum of the reversed gases to the momentum of the free-stream air flow as represented by the dimensionless parameter $-F_g/qS$. The test results shown in table II indicate that the parameter $-F_g/qS$ remains essentially constant for each reverser configuration for different values of reversed thrust and velocity at which exhaust gas ingestion occurs.

Scaling of the ingestion velocity measured in the model tests to a full-scale airplane in tables II and III was accomplished by equating

$$\left(\frac{-F_g}{q_i S}\right)_m = \left(\frac{-F_g}{q_i S}\right)_F$$

where the subscript m is for the model and the subscript F is for the full-scale airplane. For geometrically similar conditions, the ratio of reversed thrust to forward thrust remains constant, hence

$$\frac{-F_{g_m}}{F_{g_m}} = \frac{-F_{g_F}}{F_{g_F}}$$

then

$$q_{i_F} = \frac{F_{g_F}}{S_F}\left(\frac{q_{i_m} S_m}{F_{g_m}}\right)$$

Assuming that the wing area of the full-scale airplane is 2000 square feet and the four engine total thrust $F_{g_F}$ is 45,000 pounds, the velocity for ingestion of the full-scale airplane is

$$V_F = \sqrt{295\, F_{g_F} \frac{S_m}{S_F} \frac{q_{i_m}}{F_{g_m}}}$$

or

$$V_F = 1420\sqrt{\frac{q_{i_m}}{F_{g_m}}}, \text{ knots}$$

## REFERENCES

1. Tolhurst, William H., Jr., Kelly, Mark W., and Greif, Richard K.: Full-Scale Wind-Tunnel Investigation of the Effects of a Target-Type Thrust Reverser on the Low-Speed Aerodynamic Characteristics of a Single-Engine Jet Airplane. NASA TN D-72, 1959.

2. Kelly, Mark W., Greif, Richard K., and Tolhurst, William H., Jr.: Full-Scale Wind-Tunnel Tests of a Swept-Wing Airplane With a Cascade-Type Thrust Reverser. NASA TN D-311, 1960.

3. Anderson, Seth B., Cooper, George E., and Faye, Alan E.: Flight Measurements of the Effect of a Controllable Thrust Reverser on the Flight Characteristics of a Single-Engine Jet Airplane. NASA MEMO 4-26-59A, 1959.

4. Hickey, David H., and Aoyagi, Kiyoshi: Large-Scale Wind-Tunnel Tests and Evaluation of the Low-Speed Performance of a 35° Sweptback Wing Jet Transport Model Equipped with a Blowing Boundary-Layer-Control Flap and Leading-Edge Slat. NASA TN D-333, 1960.

A
4
4
5

TABLE I.- CASCADE REVERSER CONFIGURATION DETAILS

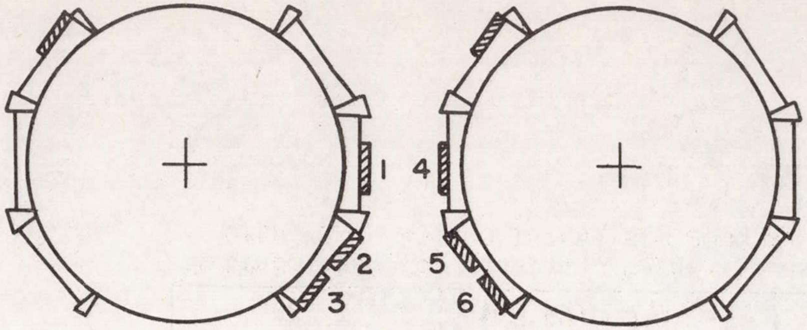


BLOCKER NUMBER SYSTEM

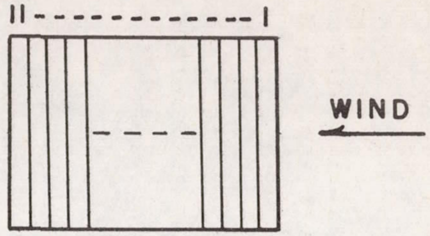


VANE NUMBER SYSTEM

| Config. No. | Inboard engine | | | | | | Outboard engine | | | | | |
|---|---|---|---|---|---|---|---|---|---|---|---|---|
| | Inboard side | | | Outboard side | | | Inboard side | | | Outboard side | | |
| | $\delta_V$, deg | | Blocker No. | $\delta_V$, deg | | Blocker No. | $\delta_V$, deg | | Blocker No. | $\delta_V$, deg | | Blocker No. |
| | 1-2 | 3-11 | | 1-2 | 3-11 | | 1-2 | 3-11 | | 1-2 | 3-11 | |
| 1 | 45 | 45 | none | 45 | 45 | none | 45 | 45 | none | 71 | 45 | none |
| 2 | 55 | 55 | ↓ | 55 | 55 | none | 55 | 55 | ↓ | 71 | 55 | ↓ |
| 3 | 45 | 45 | | 45 | 45 | 1 | 45 | 45 | | 71 | 45 | |
| 4 | 45 | 45 | | ↓ | ↓ | 1,2 | ↓ | ↓ | 4,5 | ↓ | ↓ | |
| 5 | 71 | 35 | | | | 1,2 | | | 4,6 | | | |
| 6 | ↓ | ↓ | | | | 1,3 | | | 4,6 | | | |
| 7 | | | | 55 | 55 | 1 | | | 4,6 | | | |
| 8 | 77 | | | 71 | 35 | 1,3 | 71 | 35 | 4,5 | 55 | 35 | |
| 9 | 55 | 55 | | 55 | 55 | 1,2 | 55 | 55 | 4,6 | 71 | 55 | |
| 10 | 55 | 55 | | 55 | 55 | 1,2 | 55 | 55 | 4,6 | 71 | 55 | |
| 11 | 71 | 35 | | 55 | 55 | 1 | 45 | 45 | 4 | 71 | 45 | |
| 12 | 45 | 45 | | 45 | 45 | 2 | 45 | 45 | 4,6 | 71 | 45 | |

TABLE II.- EFFECT OF REVERSED THRUST ON VARIOUS PARAMETERS

| Configuration (see table III) | $\delta_f$, deg | $F_g$, lb | $q_i$, psf | $V_i$, knots | $\Delta C_D$ at $q_\infty$ = 10 psf | $\frac{-F_g}{q_i S}$ |
|---|---|---|---|---|---|---|
| Cascade reverser No. 8 | 50 | 1,200 | 1.35 | 20 | 0.198 | 1.08 |
| | ↓ | 1,850 | 2.1 | 25 | .292 | 1.08 |
| | ↓ | 2,430 | 2.9 | 29 | .370 | 1.04 |
| | ↓ | 3,320 | 4.0 | 34 | .506 | 1.04 |
| | ↓ | 45,000[1] | --- | 49 | --- | 1.06 |
| Cascade reverser No. 9 | 0 | 1,310 | 1.0 | 17 | .186 | 1.36 |
| | ↓ | 1,850 | 1.3 | 19 | .244 | 1.38 |
| | ↓ | 2,430 | 1.7 | 22 | .304 | 1.36 |
| | ↓ | 3,340 | 2.4 | 27 | .430 | 1.40 |
| | ↓ | 45,000[1] | --- | 38 | --- | 1.38 |
| Cascade reverser No. 10 | 50 | 2,430 | 2.0 | 24 | .291 | 1.10 |
| | ↓ | 3,320 | 2.8 | 29 | .398 | 1.10 |
| | ↓ | 45,000[1] | --- | 41 | --- | 1.10 |
| Target reverser No. 1 | 50 | 2,430 | 13.2 | 62 | .228 | 1.18 |
| | ↓ | 3,020 | 16.4 | 70 | .275 | 1.20 |
| | ↓ | 45,000[1] | --- | 104 | --- | 1.20 |

[1]Extrapolated for constant $F_g/qS$ to assumed full-scale airplane with $F_g$ = 45,000 lb and S = 2000 sq ft

TABLE III.- RESULTS OF THE CONFIGURATION CHANGES ON THE CASCADE AND TARGET-TYPE THRUST REVERSERS; $\delta_f = 50^\circ$

(a) Cascade reverser

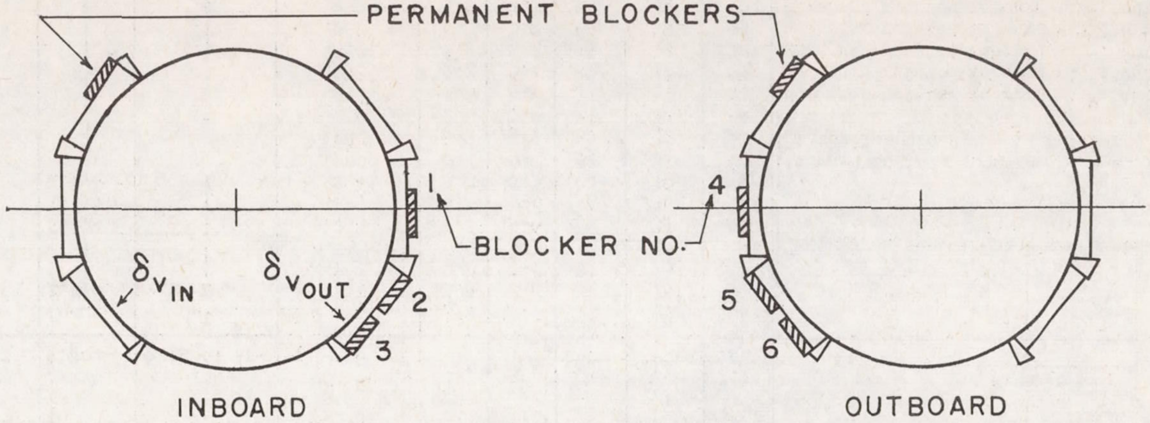


| No. | $\delta_V$ Nominal, deg | Blocker No. | $\Delta C_D$ at $q_\infty$ = 10 psf | $q_{i_m}$ | $q_{t_m}$ | $V_{im}$, knots | $V_{tm}$, knots | $V_{i_f}$ (1) | Remarks |
|---|---|---|---|---|---|---|---|---|---|
| 1 | 45 | None | 0.336 | 8.5 | 8.2 | 50 | 49 | 84 | |
| 2 | 55 | None | .295 | 7.0 | 6.8 | 45 | 44 | 76 | |
| 3 | 45 | 1,4 | .354 | 8.6 | 3.4 | 51 | 32 | 84 | |
| 4 | | 1,2,4,5 | .346 | 3.2 | 3.1 | 31 | 30 | 52 | |
| 5 | | 1,2,4,6 | .336 | 2.6 | 2.3 | 28 | 26 | 46 | |
| 6 | | 1,3,4,6 | .324 | 3.1 | 3.0 | 30 | 30 | 51 | |
| 7 | | 1,4,6 | .356 | 3.1 | 2.3 | 30 | 26 | 51 | |
| 8 | 35 | 1,3,4,5 | .370 | 2.9 | 2.1 | 29 | 25 | 49 | |
| 9[2] | 55 | 1,2,4,6 | .304 | 1.7 | 1.4 | 22 | 20 | 38 | |
| 10 | 55 | 1,2,4,6 | .291 | 2.0 | 1.8 | 24 | 23 | 41 | |
| 11 | 45 | 1,4 | .376 | 5.2 | 3.5 | 39 | 32 | 65 | $\delta_{vin} = 35^\circ$; $\delta_{vout} = 55^\circ$ |
| 12 | 45 | 2,4,6 | .324 | 1.2 | 1.2 | 19 | 19 | 32 | Canted vanes |

[1]Extrapolated for constant $F_g/qS$ to $F_g$ = 45,000 lb and S = 2,000 sq ft

[2]Configuration No. 9 $\delta_f = 0^\circ$

TABLE III.- RESULTS OF THE CONFIGURATION CHANGES ON THE CASCADE AND TARGET-TYPE THRUST REVERSERS; $\delta_f = 50^{\circ}$ - Concluded

(b) Target-type reverser

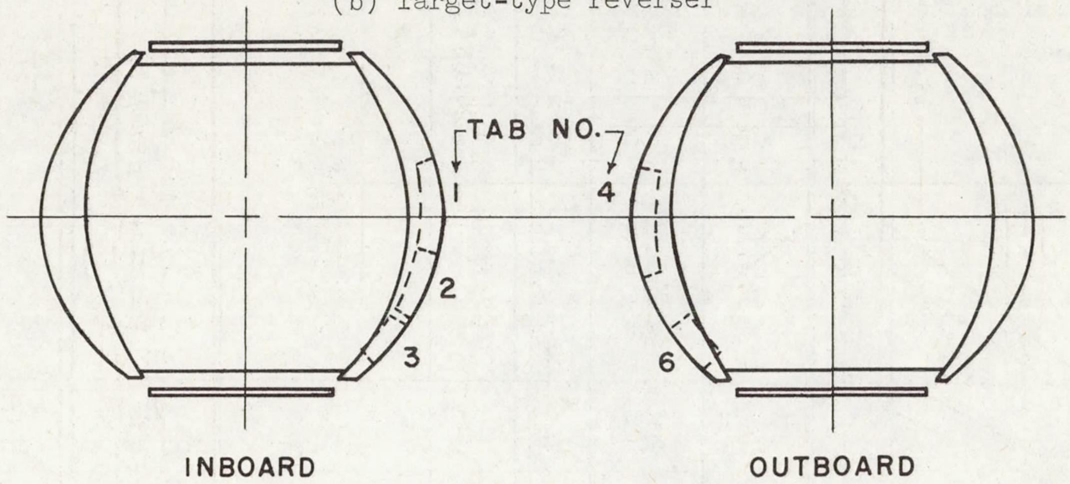


| No. | $\delta_v$ nominal, deg | Tab No. | Tab height, in. | $\Delta C_D$ at $q_\infty$ = 10 psf | $q_{i_m}$ | $q_{t_m}$ | $V_{i_m}$, knots | $V_{t_m}$, knots | $V_{i_f}$ (1) | Remarks |
|---|---|---|---|---|---|---|---|---|---|---|
| 1 | 30 | none | --- | 0.228 | 13.2 | 11.7 | 62 | 59 | 104 | |
| 2 | 25 | 1,4,6 | 2 | .258 | 5.4 | 3.6 | 40 | 33 | 67 | Inboard engine, inboard end plate off |
| 3 | 30 | ↓ | ↓ | .263 | 5.2 | 3.6 | 39 | 33 | 66 | |
| 4 | 35 | ↓ | ↓ | .238 | 5.0 | 4.3 | 38 | 35 | 64 | |
| 5 | ↓ | 1,2,4,6 | ↓ | .230 | 5.2 | 4.6 | 39 | 37 | 66 | |
| 6 | ↓ | 1,3,4,6 | ↓ | .239 | 5.8 | 5.8 | 41 | 41 | 70 | |
| 7 | 30 | 1,4,6 | ↓ | .294 | 5.8 | 5.5 | 41 | 40 | 70 | Inboard engine, inboard $\delta_v$ = 25°; reversers tilted inboard 4.1° up, outboard 3.3° down |
| 8 | ↓ | ↓ | 1 | .250 | 8.7 | 8.7 | 51 | 51 | 85 | |
| 9 | ↓ | ↓ | 2 | .268 | 4.3 | 3.9 | 35 | 34 | 60 | |
| 10 | ↓ | ↓ | 3 | .218 | 2.0 | 1.6 | 24 | 22 | 41 | |
| 11 | ↓ | ↓ | 2 | .278 | 4.6 | 4.6 | 37 | 37 | 62 | Reverser rotated inboard +15°; outboard 0° |
| 12 | ↓ | ↓ | ↓ | .238 | 5.3 | 5.1 | 39 | 38 | 67 | Reverser rotated inboard +15°; outboard +15° |
| 13 | ↓ | ↓ | ↓ | .250 | 6.3 | 6.3 | 43 | 43 | 72 | Reverser rotated inboard -15°; outboard +15° |
| 14 | ↓ | ↓ | ↓ | .268 | 8.2 | 8.2 | 49 | 49 | 83 | Reverser rotated inboard -15°; outboard -15° |
| 15 | ↓ | ↓ | ↓ | .279 | 5.5 | 4.1 | 40 | 40 | 68 | Reverser rotated inboard +15°; outboard -15° |
| 16 | 35 | none | --- | .232 | 8.4 | 6.8 | 50 | 45 | 84 | Finned end plate |
| 17 | 30 | none | --- | .212 | 3.8 | 2.3 | 33 | 26 | 56 | Tapered end plate |
| 18 | 30 | 1,4,6 | 2 | .225 | 1.9 | 0 | 23 | 0 | 40 | |

[1]Extrapolated for constant $F_g/qS$ to $F_g$ = 45,000 lb and S = 2,000 sq ft

A
4
4
5

Wing

| | |
|---|---|
| Aspect ratio | 7.0 |
| Taper ratio | 0.3 |
| Area | 302.0 sq ft |
| Mean aerodynamic chord | 7.2 ft |
| Dihedral | 6.0 deg |

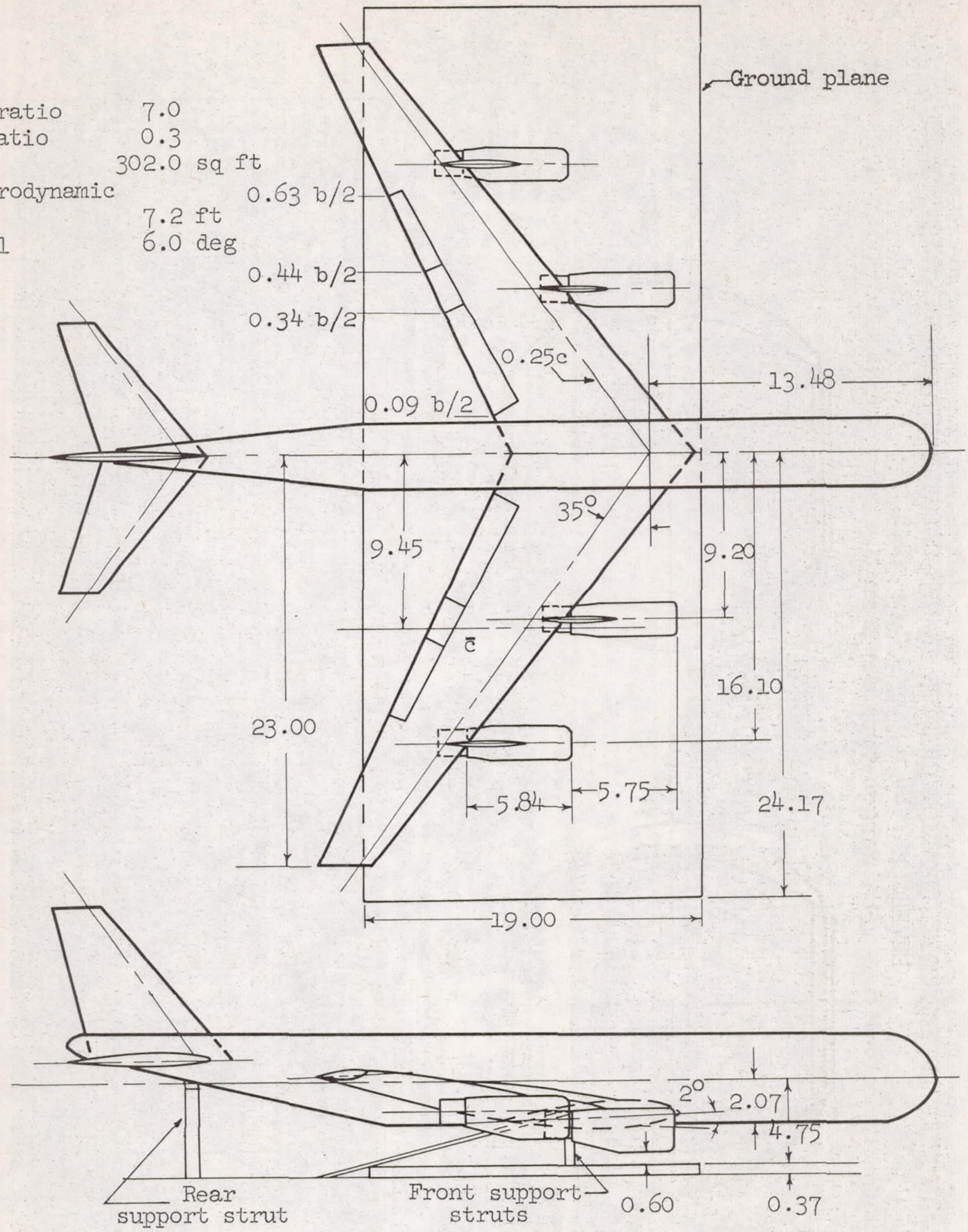


Figure 1.- Model dimensions (in feet except as noted).

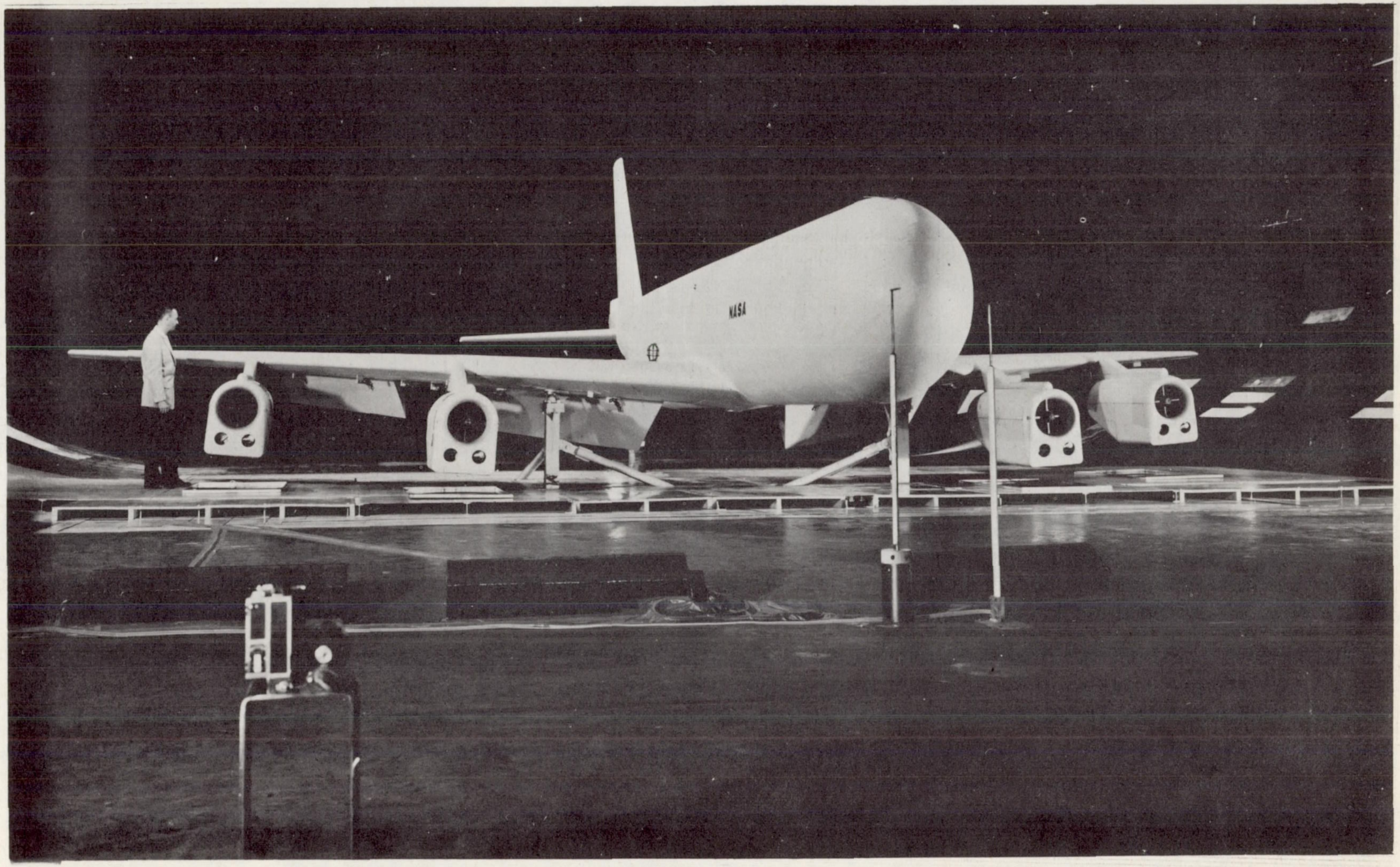


A-25244

Figure 2.- Photograph showing model installation in Ames 40- by 80-Foot Wind Tunnel.

A445

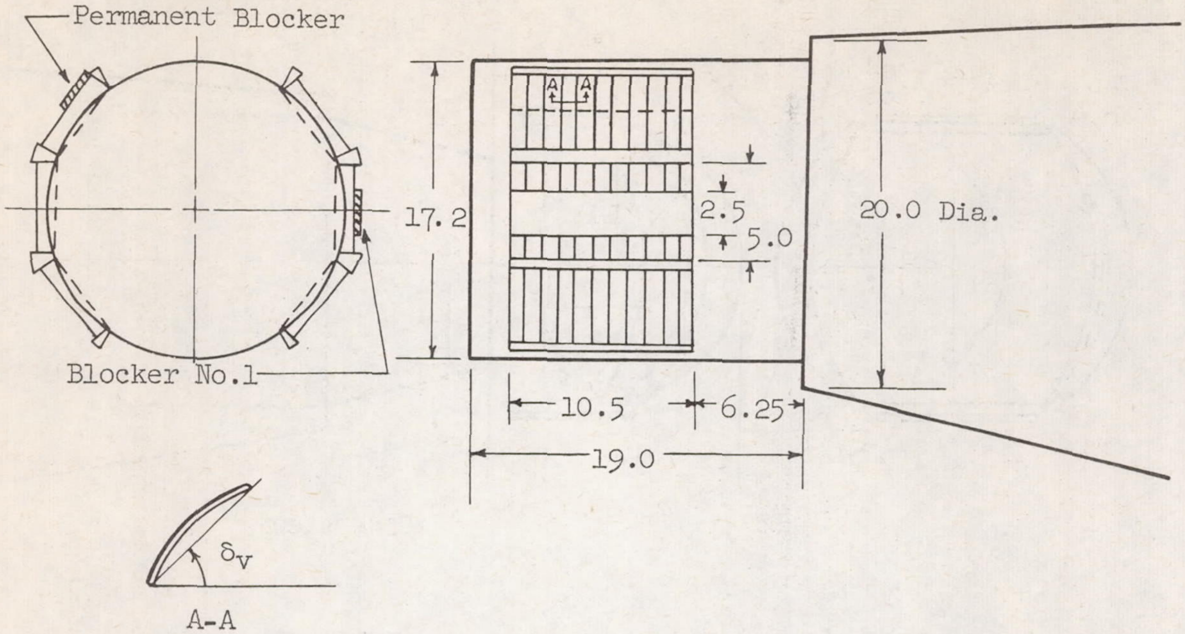


(a) Basic configurations showing blocker plate No. 1 and permanent blocker. (Dimensions in inches)

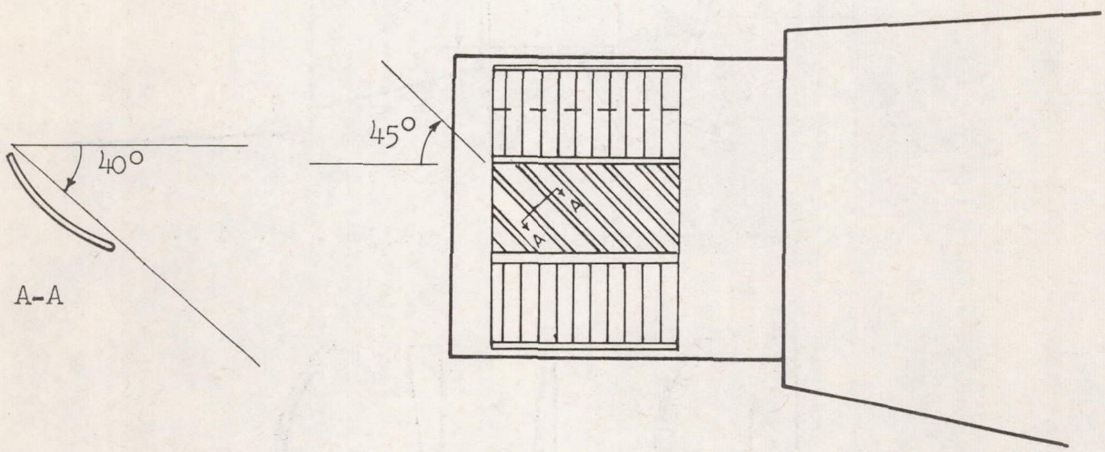


(b) Canted vane configuration.

Figure 3.- Details of cascade reverser.

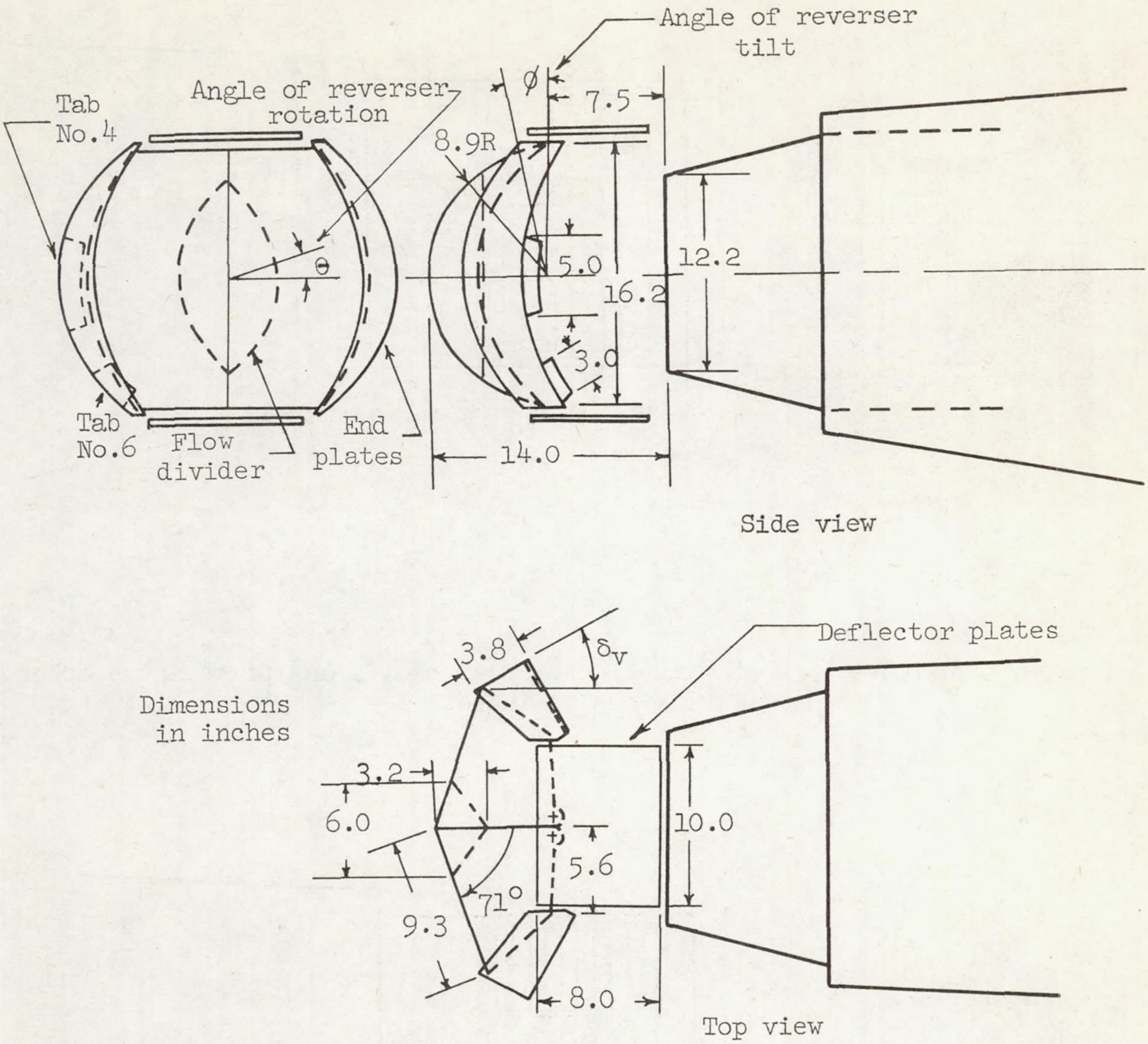


(a) Basic configuration showing tabs Nos. 4 and 6.

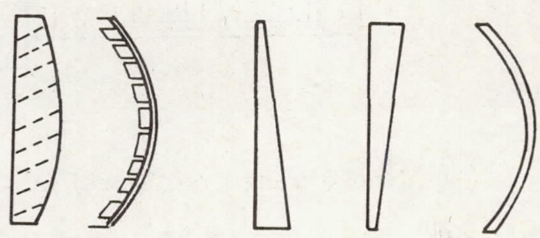


(b) Alternate end-plate configurations.

Figure 4.- Details of target reverser.

A
4
4
5

A445

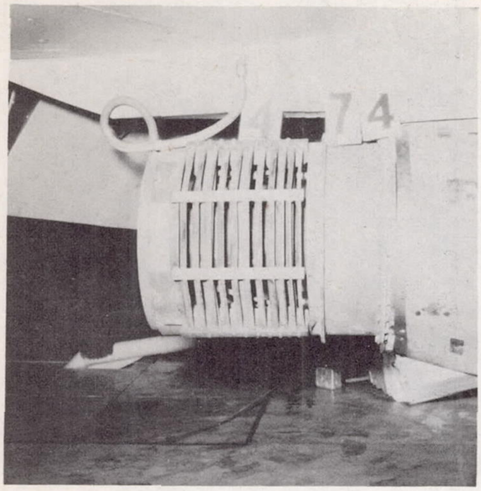

Plain reverser

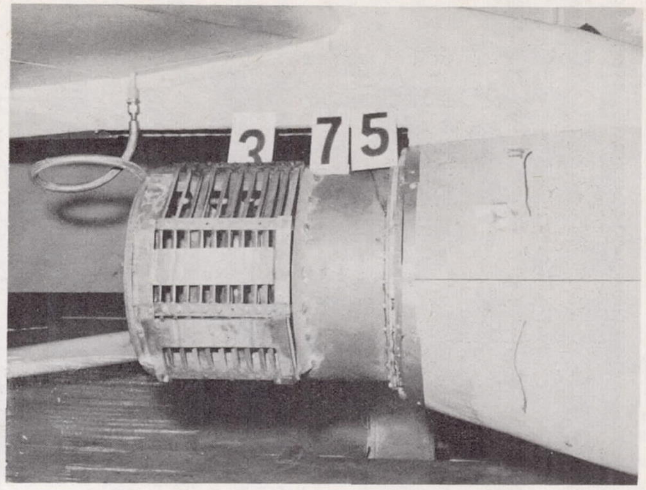


Reverser with blocker 1 and 2

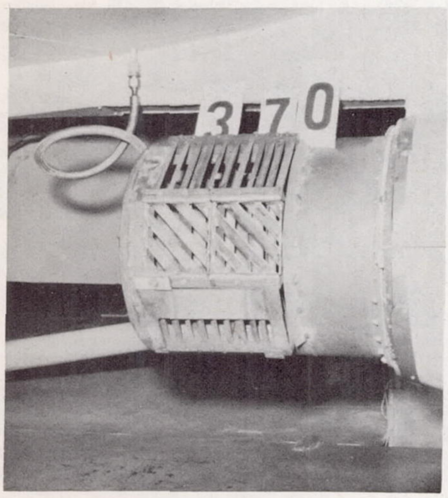

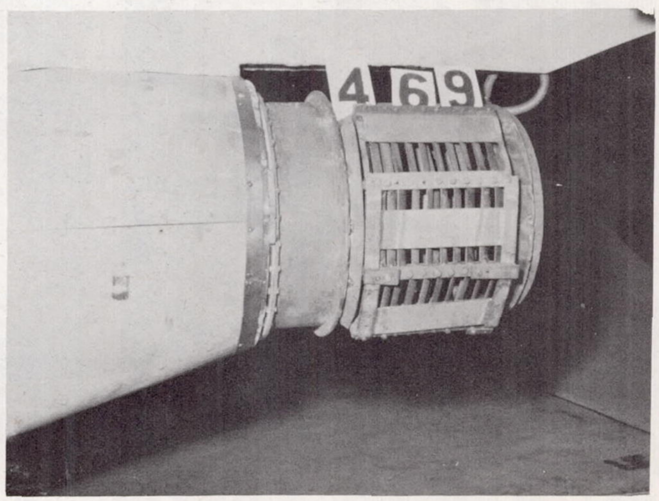


A-27117

Canted vane installation

(a) Cascade reverser.

Figure 5.- Photographs of various reverser installations.

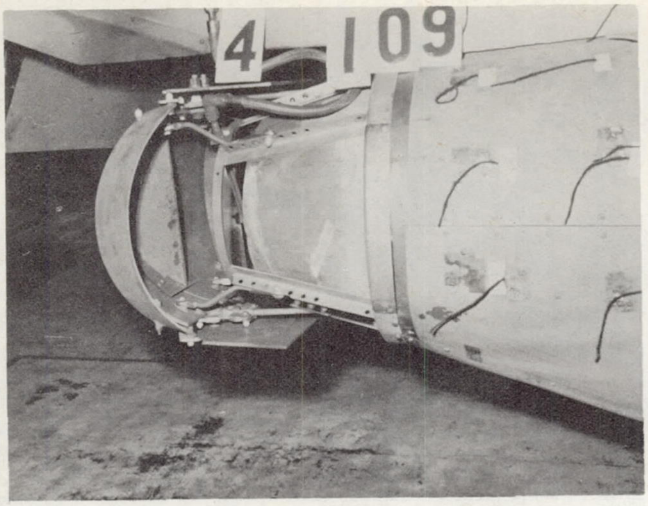


Plain end plate


End plate with tabs 1 and 3

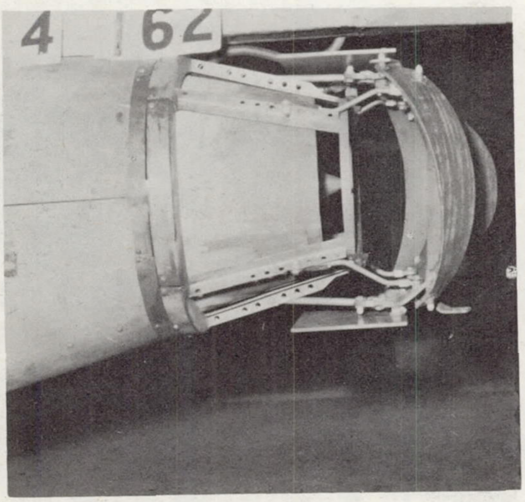


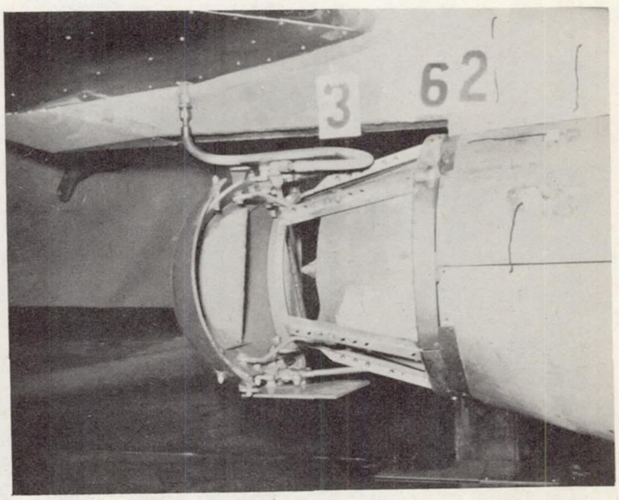


A-27116

Tapered end plates

(b) Target reverser.

Figure 5.- Concluded.

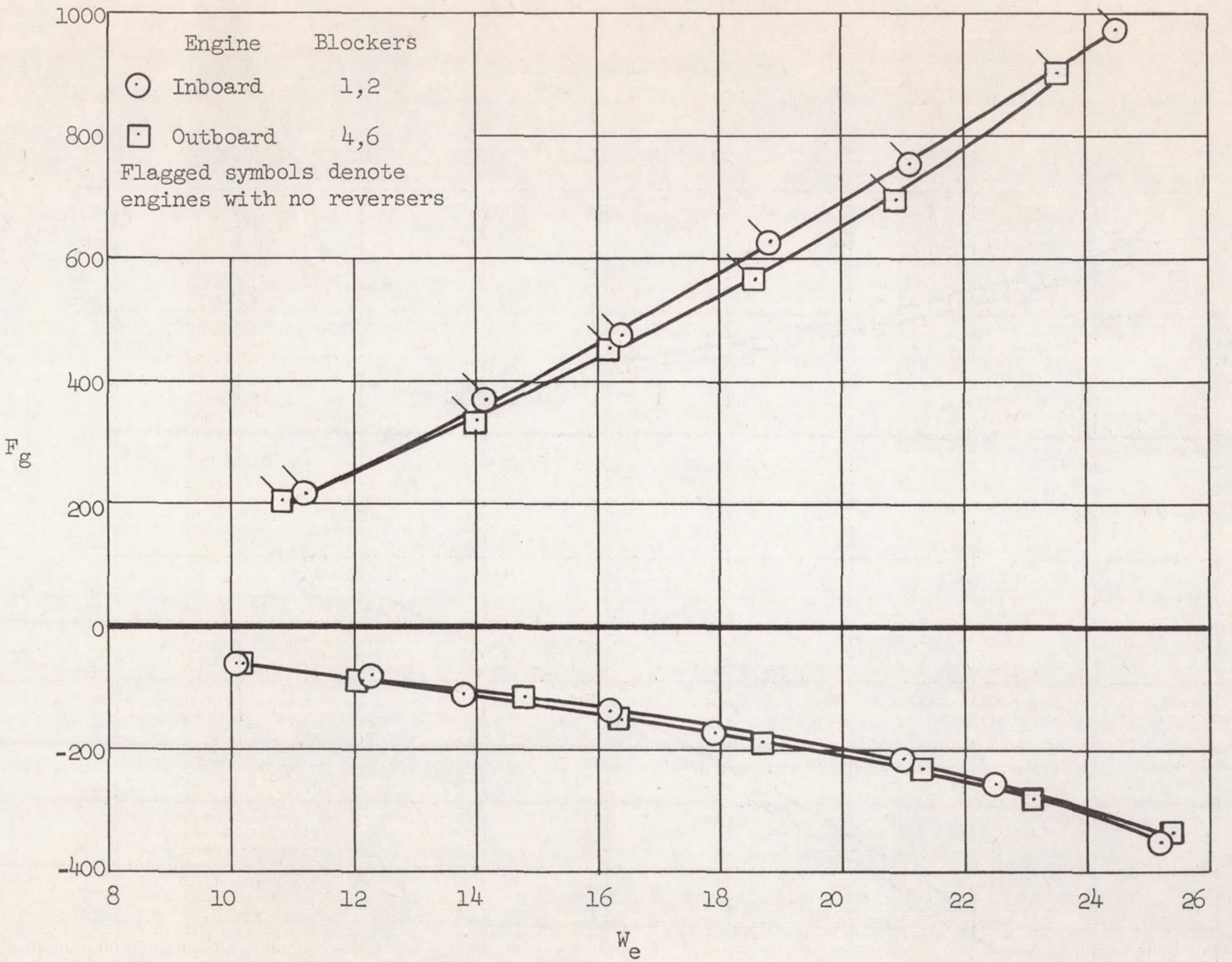


(a) Cascade reverser, $\delta_v = 55^\circ$.

Figure 6.- Variation of gross thrust with corrected engine weight rate of flow for each engine with and without reversers; $\delta_f = 0^\circ$, $q_\infty = 0$.

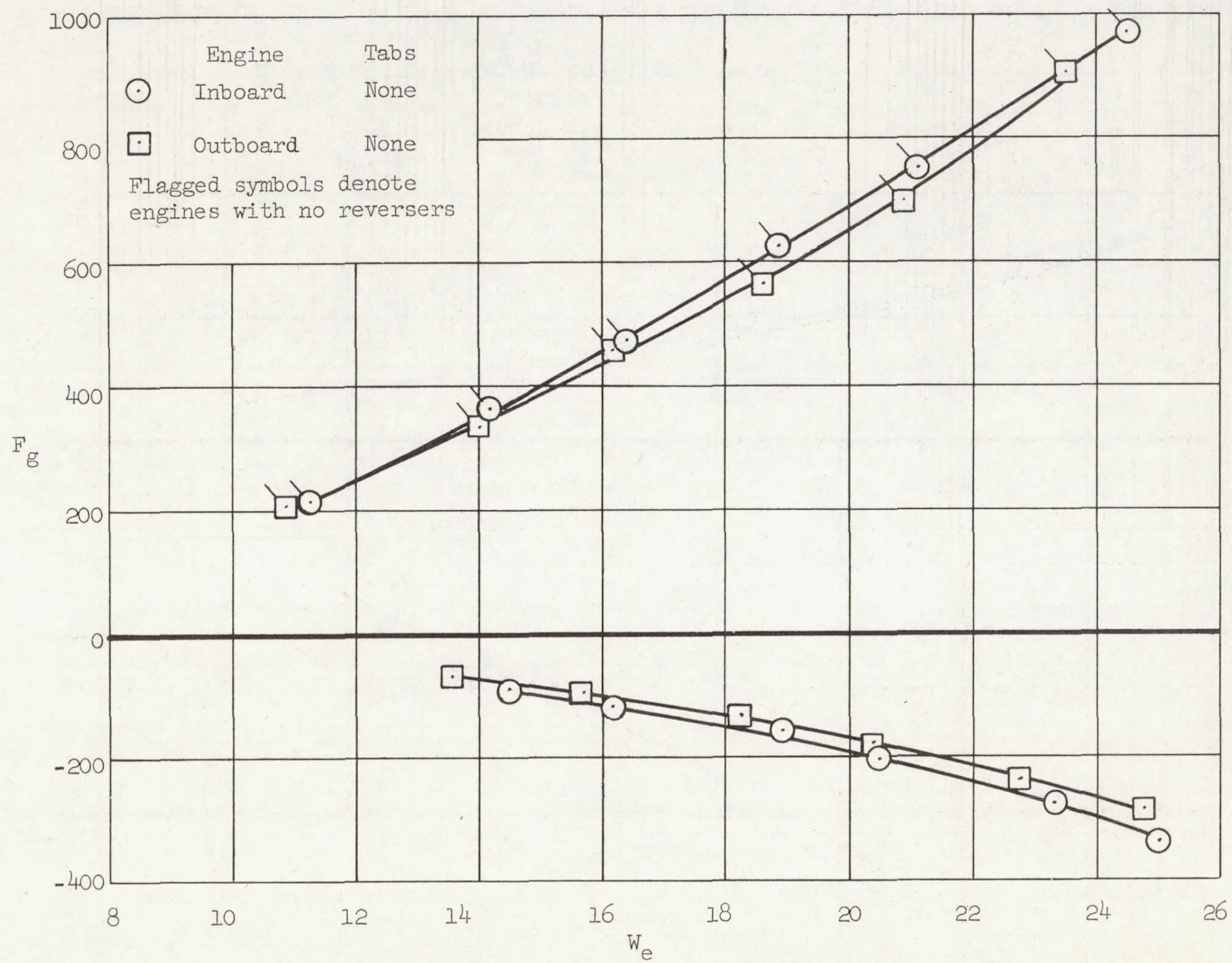


(b) Target reverser, $\delta_V = 30^{\circ}$.

Figure 6.- Concluded.

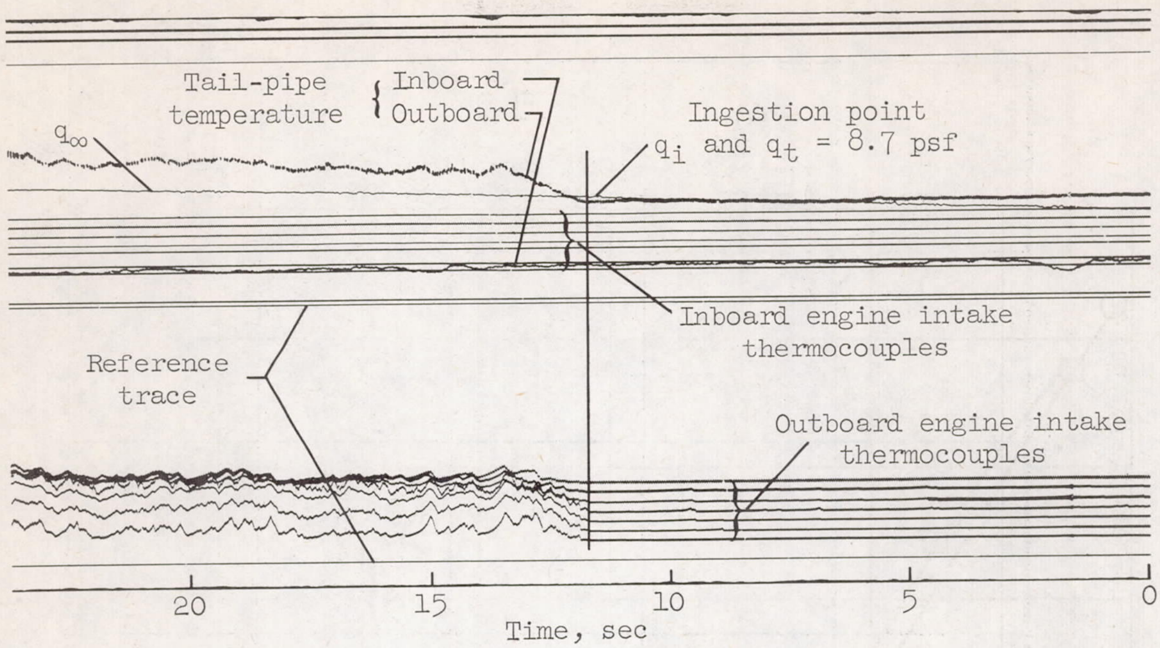


(a) Target configuration No. 8.

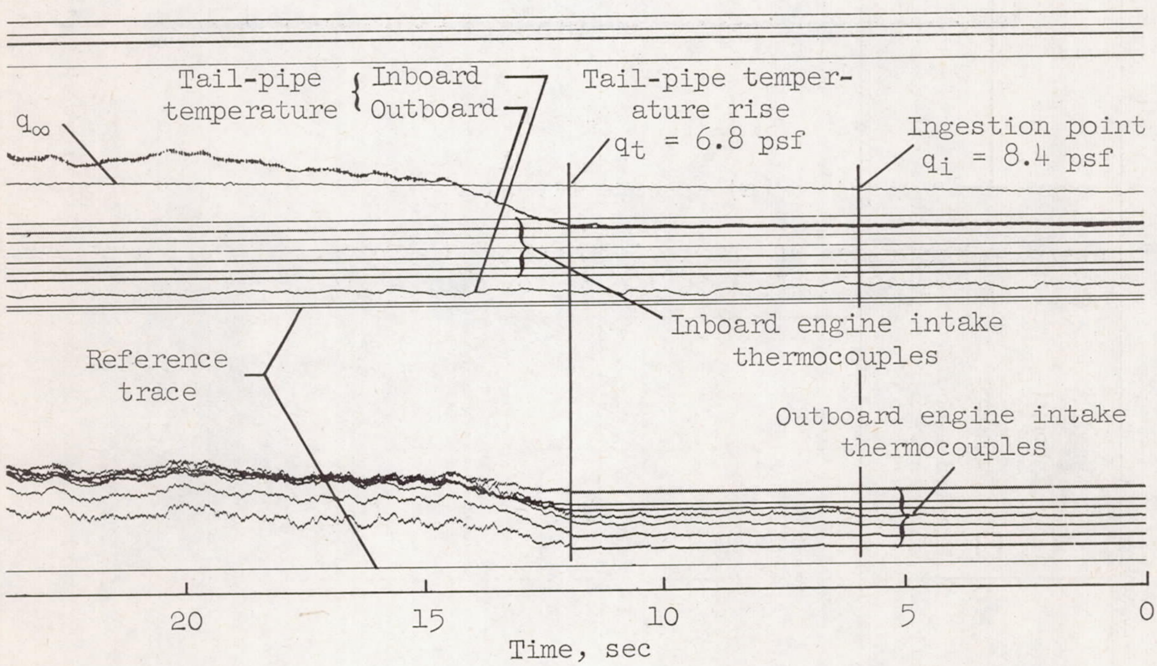


(b) Target configuration No. 16.

Figure 7.- Typical oscillograph records showing two types of exhaust gas ingestion as indicated by the intake and tail-pipe thermocouples.

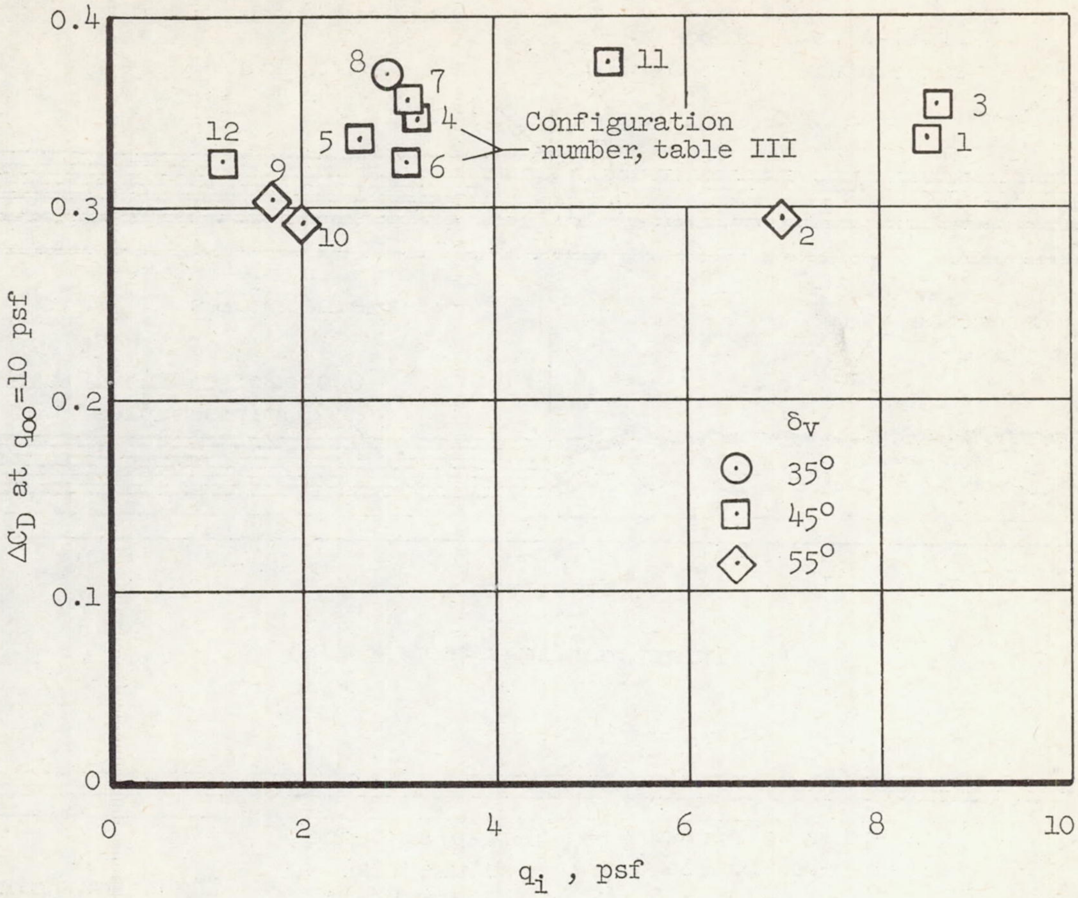


(a) Cascade reverser.

Figure 8.- Comparison of the performance of the reverser configurations; $F_g$ = 2430 lb, $\delta_f$ = 50°; $\Delta C_D$ for four engine operation.

A
4
4
5

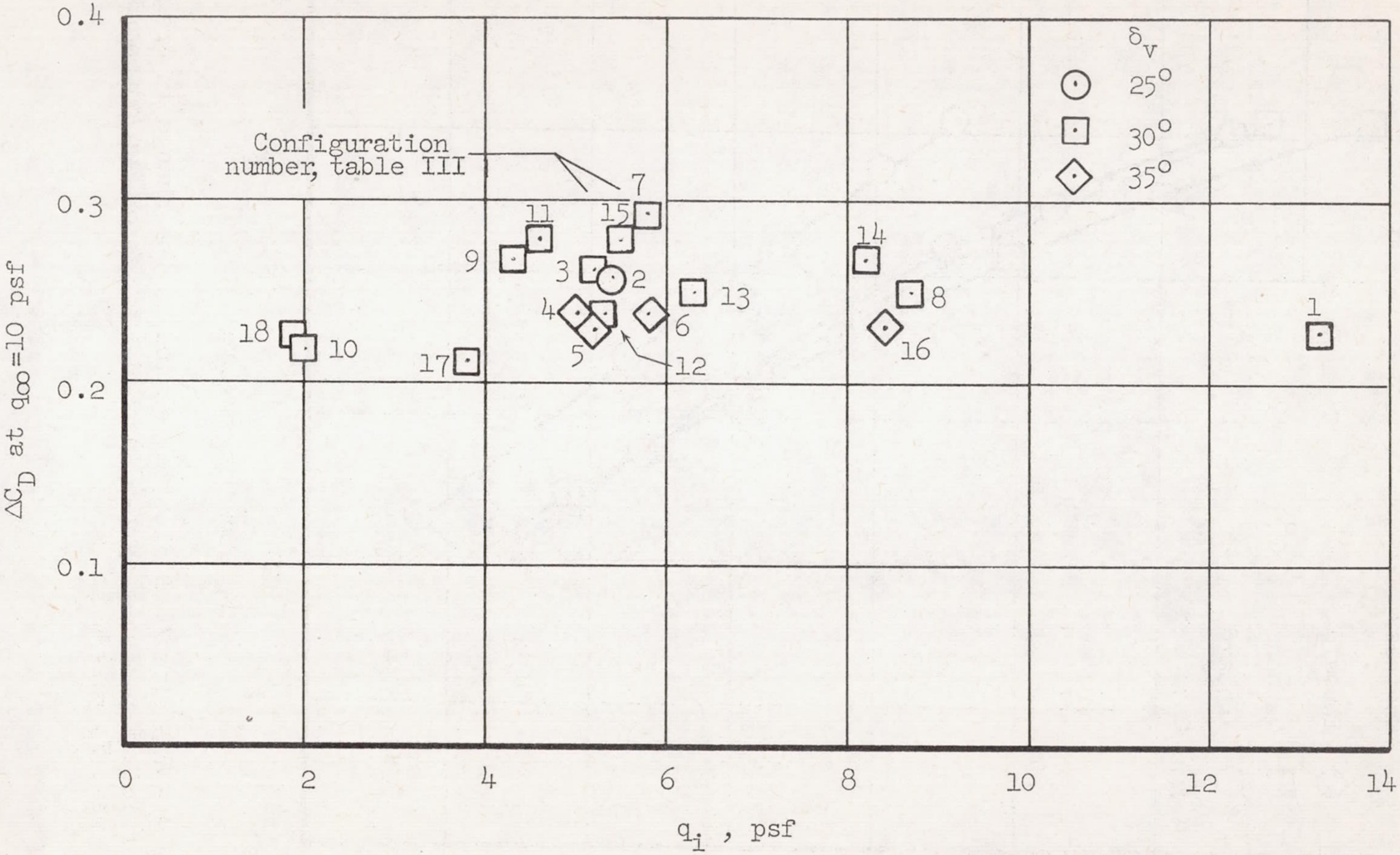


(b) Target reverser.

Figure 8.- Concluded.

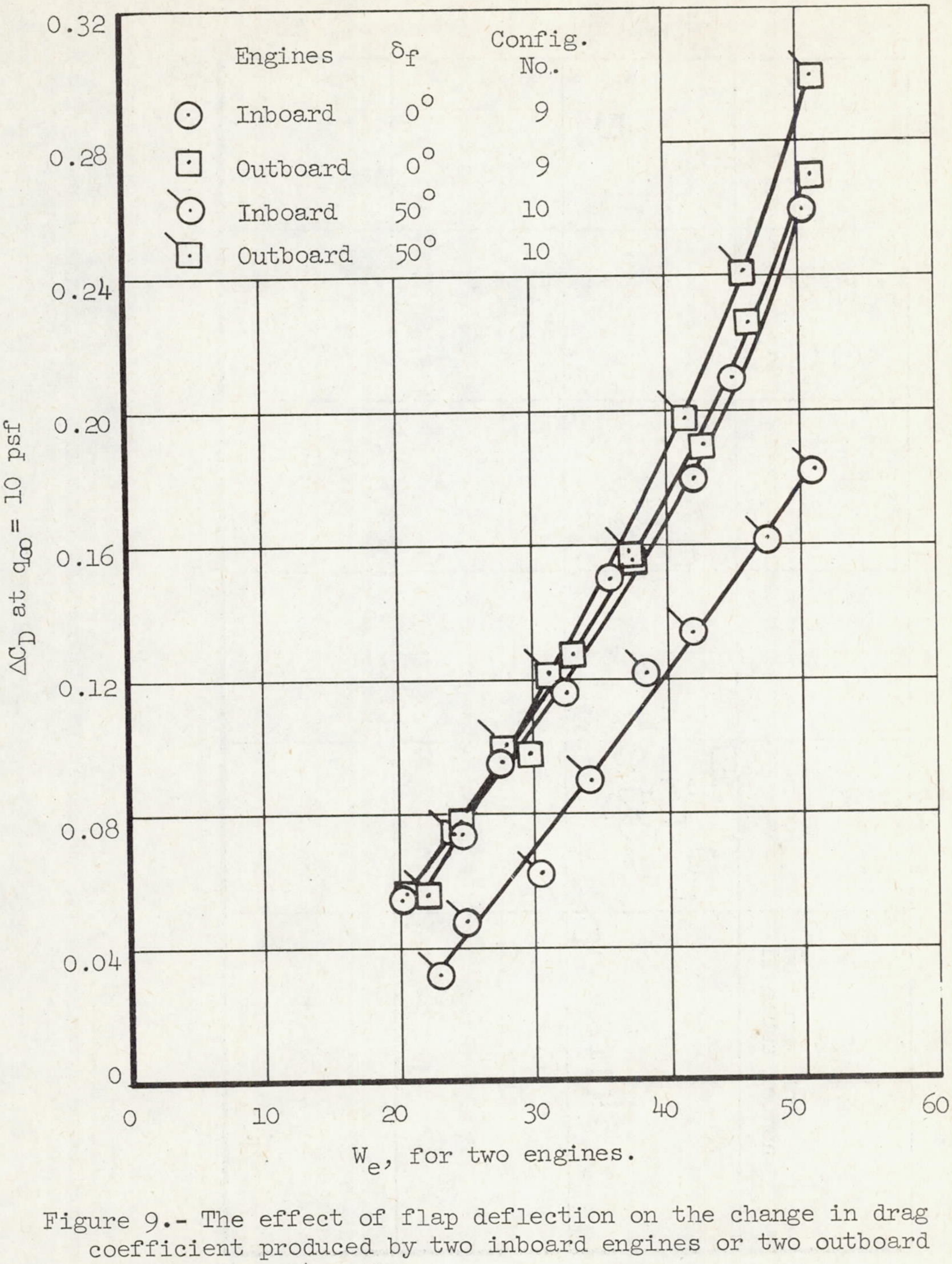


Figure 9.- The effect of flap deflection on the change in drag coefficient produced by two inboard engines or two outboard engines; $F_g = 2430$ lb.

A
4
4
5